JOM, Vol. 72, No. 12, 2020
https://doi.org/10.1007/s11837-019-03851-8

Coatings Corrosion Resistance of Poly(*o*-Phenylenediamine) on Mild Steel in 3.5% NaCl: Influence of Inorganic Acid

JIA-WEI ZHANG,[1] YING LI,[1,2] YU-SHI DING,[1] KE-FENG PAN,[1] and QING ZHAO[1]

1.—School of Metallurgy, Northeastern University, Shenyang 110819, China. 2.—e-mail: liying@mail.neu.edu.cn

Poly(*o*-phenylenediamine) was synthesized in different inorganic acid media, hydrochloric (HCl), nitric (HNO_3), and phosphoric acid (H_3PO_4). The aim was to investigate the protective effect of doped coatings on mild steel in an aggressive environment. The synthesized doped-PoPD products were characterized by x-ray diffractometry, Fourier transform infrared spectroscopy, scanning electron microscopy, and cyclic voltammetry. The inhibition abilities of doped coatings were evaluated by potentiodynamic polarization measurements and electrochemical impedance spectroscopy in 3.5% NaCl solution. In the present article, the lowest corrosion current and highest protection efficiency of the doped polymer were observed for the polymer synthesized in HNO_3 medium. The results showed that good protection of mild steel can be achieved by PoPD coating doped with inorganic acid in 3.5% NaCl solution.

INTRODUCTION

Mild steel (MS) is the primary metal used for different infrastructures because of its good performance and ease of manufacturing.[1] It is not only used for construction of houses, bridges, and railways and in different industries manufacturing machinery, but is also used in the modern petrochemical industries, rigging industry, etc. However, mild steel is susceptible to localized corrosion, which leads to a decrease in structural integrity and loss of mechanical properties. Moreover, high-alloy steels have certain probability of getting eroded in highly corrosive solutions.[2] Therefore, localized corrosion of mild steel is one of the problems considered during the application of mild steel. Corrosion inhibitors or coatings are generally used for the protection of MS from corrosion.[3]

Application of π-conjugated conductive polymers (CPs), such as polyaniline, polypyrrole, and polyurethane, as components of corrosion-resistant coatings, continues to generate considerable interest.[4–6] The CP coatings in conductive form have more positive potentials than iron and aluminum, so they can protect these metals in a corrosive environment and serve as an alternative to the non-environmentally friendly chromate films.[7,8] DeBerry reported that polyaniline (PANI) coatings provide anodic protection for stainless steel. PANI significantly transforms the component, forms a passive film on stainless steel (Ss), and significantly reduces the corrosion rate.[5] The formation of a passivation film is usually the result of a coupling process in a redox state between the active metal and conductive polymer.[9]

The relationship between the special structure of organic compounds and their inhibition of corrosion has been studied extensively.[10] These studies have shown electronegative atoms (such as N, S, and P), unsaturated bonds (double or triple bonds), and planar conjugate systems of various aromatic rings to be most effective for corrosion inhibition. The significant reduction in corrosion rate can be attributed to the fact that the above structures provide active electrons or empty orbitals to provide or receive electrons.[3]

Investigations on aromatic diamine polymers have received considerable attention because of their advantages of functionality, photocatalytic activity, supercapacitance, multi-color electrochromism, and indication of fluorescence, which are precursors for the synthesis of carbon materials, their biologic applications, environmental stability, and thermal stability.[11–16] Poly(*o*-phenylenediamine) (PoPD) has a long-chain ladder-like structure, similar to polyaniline quinone molecules.

(Published online October 21, 2019)

Polymerization occurs by substitution of 1 and 4 positions on the benzene ring with the amino groups of another molecule of o-phenylenediamine. However, the electrochemical properties of PoPD and PANI are significantly different.[17] According to Ganash et al., PANI films on Ss showed lower corrosion resistance than PoPD films. Since PANI layers are more porous and have higher ionic conductivity, their barrier efficiency is lower than that of PoPD.[18]

Porosity and anion exchange properties of CPs reduce corrosion resistance and cause pitting of metals, especially in small aggressive anionic environments such as in the presence of chlorides.[19] According to Düdükcü, the PoPD coating could strongly adhere to the metal surface and prevent the corrosion of Ss by anodic protection.[4] However, on increasing its time of immersion in 3.5% NaCl, the corrosion protection of PoPD decreased. By doping of different organic or inorganic acids into the polymer, the protective properties of the conductive polymer can be increased.[11,20–22] Samanta et al.[11,22] investigated the effect of different structures on the conductivity of the synthesized polymers incorporated with different inorganic acid dopants. Their study showed that the conductivity of the doped PoPD was improved by the protonation "induced doping" of =NH side groups. The direct current conductivities of HCl- and H_2SO_4-doped PoPD films were increased to 6.98×10^{-5} S/cm^{-1} and 1.16×10^{-3} S/cm^{-1}, respectively, compared with that of undoped PoPD (1.21×10^{-6} S/cm^{-1}). Few studies have been conducted on the corrosion resistance of PoPD layers doped with different inorganic acids in an environment containing corrosive chlorine anions, especially the one doped with dilute nitric acid.

The main objectives of the present work are as follows: (1) to synthesize poly(*o*-phenylenediamine) with different acids as dopants (HCl, HNO_3, and H_3PO_4) and (2) to investigate the corrosion performance of doped-poly(*o*-phenylenediamine) coating on mild steel. For this purpose, the corrosion behaviors of the polymer-coated and uncoated mild steel were investigated in 3.5% NaCl solution at room temperature. Potentiodynamic polarization measurements and electrochemical impedance spectroscopic measurements of the coatings were evaluated and compared.

EXPERIMENTAL

Materials

o-Phenylenediamine monomer (98% purity) was purchased from Beijing Infinity. Ammonium persulfate (98.5% purity) was procured from Aladdin. Ethyl acetate (99.5% purity), phosphoric acid (98% purity), and nitric acid (70% purity) were obtained from Tianjin Kemiou. Hydrochloric acid (37.5 wt.%) was purchased from XiLong Chemical. *N*-methyl-2-pyrrolidone was obtained from Damao Chemical (99%). Waterborne polyurethane and hexamethylene diisocyanate were procured from BOMEX. Ethanol was purchased from Sinopharm Chemical. All raw materials were used without any further purification.

Preparation of Polymer Powders and Coatings

Poly(*o*-phenylenediamine) (PoPD) was synthesized by in situ emulsion polymerization, in which HCl and the monomer, *o*-phenylenediamine, were reacted in 1:1 molar ratio. The general procedure for preparation of PoPD by emulsion polymerization is as follows: First, aqueous solution of HCl was added into *o*-phenylenediamine (5.4 g) under magnetic stirring. Then, ammonium persulfate solution (1 M, 50 mL) was added drop-wise to the above mixture and was stirred at < 10°C for at least 12 h to complete the reaction. Thereafter, the precipitate was filtered and washed with distilled water and ethanol. The washed precipitate was dried in a vacuum oven at 60°C for 24 h to obtain HCl-doped PoPD. Similarly, HNO_3- and H_3PO_4-doped PoPD was also prepared by using HNO_3 and H_3PO_4, respectively, instead of HCl.

The carbon specimens with dimensions of 2 cm × 2 cm were mechanically polished with SiC papers (grades 800 and 1000), followed by washing and degreasing with acetone and double distilled water, and finally dried in air. The as-prepared powder (0.2 g) was suspended in NMP (0.4 mL) and ethyl acetate (0.2 mL). Waterborne polyurethane and the curing agent, HDI, in a mass ratio of 10:1 were added to the above solution, stirred, and then sonicated until no bubbles were formed. It was then applied to the surface of the steel sample. An AIRAJ micrometer was used to measure the thickness of the layer, which was found to be about 115 μm. The substrates were subjected to the above treatment prior to any experiments and were used without further storage.

Characterization

The structures of the samples were characterized by Fourier transform infrared spectroscopy on a Nicolet 380 FT-IR, Thermo Electron Corp., in the spectral range of 4000–500 cm^{-1}. The x-ray diffraction (XRD) patterns of the samples were obtained using a Smart Lab x-ray diffractometer from Rigaku Corp., which operated at 45 kV/200 mA in the 2θ range of 10°–90° with a Cu K-α irradiation source. The powder morphologies of the samples were investigated by scanning electron microscopy using a SU 8010 from Hitachi. Cyclic voltammetry (CV), potentiodynamic polarization, and electrochemical impedance spectroscopic (EIS) measurements were carried out using a CHI660E electrochemical workstation. Cyclic voltammetry was carried out using carbon paper in 1.0 M HCl solution at a sweep rate of 100 mV/s in the range of -0.6 V to 0.2 V.

Polarization curves were obtained at a sweep rate of 1 mV/s in the range of − 1.0 V to 1 V (vs. SCE). EIS measurements were performed using CHI660E with 5 mV amplitude in the frequency range of 10^5 Hz to 0.01 Hz, and Zview 2.0 software was used to fit the equivalent circuit of EIS data.

RESULTS AND DISCUSSION

Analysis of Structures, Morphologic and Cyclic Voltammetry Test

The FTIR spectra of hydrochloric acid-doped poly(*o*-phenylenediamine) and PoPD polymers doped with different inorganic acids are shown in Fig. 1. In Fig. 1a peaks at 3400 cm^{-1} and 3200 cm^{-1} correspond to the stretching vibrations of $–NH_2$ and =NH, respectively.[22,23] The peak at 1690 cm^{-1} was attributed to C=N vibrations in the polymer. Peaks at 1640 cm^{-1} and 1525 cm^{-1} were characteristic of the free =NH group and C=C of the aromatic ring.[11,18,22,23] The 1370 cm^{-1} and 1240 cm^{-1} peaks could be attributed to C–N stretching vibrations of the aromatic ring.[19,23] The peaks around 830 cm^{-1} and 760 cm^{-1} were ascribed to the 1,2,4-trisubstituted benzene ring,[24,25] whereas the peak at 620 cm^{-1} was attributable to the toroidal deformation.[18] The above data were consistent with the literature data, which proposed a ladder structure of a polymer containing a phenazine ring with an asymmetrical quinone ring structure.[18] Therefore, the structures of polymers synthesized in HCl and H_3PO_4 media were consistent with those reported in the literature.[11] The characteristic peaks in the 1800–900 cm^{-1} region could be attributed to protons formed during the polymerization reaction. Two characteristic vibrational peaks for HPO_4^{2-} and $H_2PO_4^-$ appeared at 1110 cm^{-1} and 810 cm^{-1}, respectively, for the polymer synthesized in H_2PO_4.[26–28] The peak at 1239 cm^{-1} corresponded to $C–N^+$ stretching in the polaronic form of polymer salt.[29]

Figure 1b shows the XRD patterns of PoPD doped with different inorganic acids such as hydrochloric, nitric, and phosphoric acids. The XRD patterns of PoPD doped with different inorganic acids showed sharp peaks in the range of 2θ = 10°–29°, indicating the partially crystalline nature. In general, the peak at around 2θ = 20° was attributed to the periodic distance between the dopant and nitrogen on the adjacent polymer chain.[24] The diffraction peak at 2θ = 26.5° was characteristic of the polymer, and the localized crystallinity could be attributed to the addition of acid dopant or periodicity perpendicular to the polymeric chain.[23,30–33]

Cyclic voltammetry (CV) is a comprehensive electroanalytical technique for studying the redox properties and their reversibility in polymers. When CV is employed for studying electropolymerization, the number of electrons involved in the redox reaction and degradation of conductive polymers can also be analyzed. The cyclic voltammograms of freshly prepared PoPD–HCl, PoPD–HNO_3, and PoPD–H_3PO_4 powders on carbon paper in 1 M HCl solution, recorded in the potential range of E_{SCE} = − 0.6–0.2 V at a scan rate of 100 mV/s, are shown in Fig. 2a. PoPD–HCl and PoPD–H_3PO_4 exhibited peaks corresponding to electrochemical oxidation at − 0.080 V and − 0.078 V (vs. SCE) and those corresponding to electrochemical reduction at − 0.169 V and − 0.160 V (vs. SCE), respectively. Two oxidation peaks were observed for PoPD–HNO_3 at − 0.102 V and 0.124 V. Moreover, PoPD–HNO_3 did not show any significant reduction peak.

The cyclic voltammograms were highly reproducible after multiple cycles, as shown in Fig. 2b, which indicated cycling stability. CVs of samples in Fig. 2b did not show any other peak. This indicated that PoPD–HCl, PoPD–HNO_3, and PoPD–H_3PO_4 were collected in pure form after synthesis. It also showed a more stable electroactivity and lesser degree of degradation.

The SEM images of PoPD–HCl, PoPD–HNO_3, and PoPD–H_3PO_4 coatings are shown in Fig. 3. The surface of PoPD–HCl in Fig. 3a showed the distribution of a large number of flakes and particles. The structure as a whole had an irregular shape and a

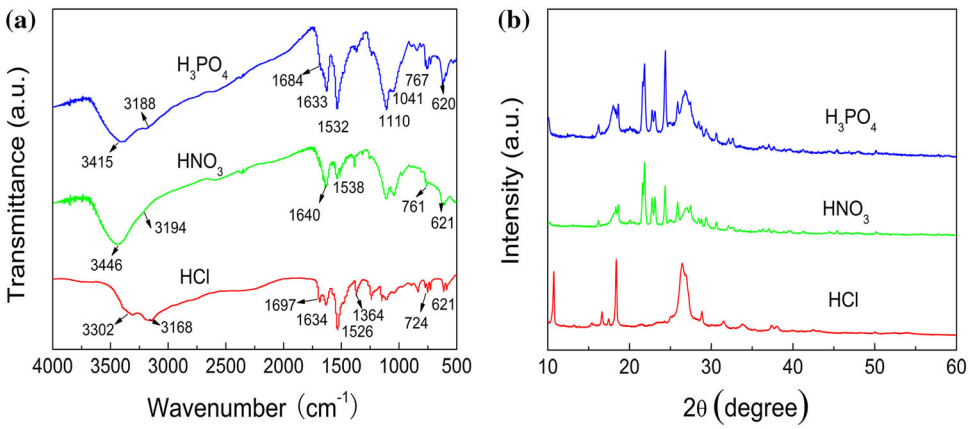

Fig. 1. Structure analysis of different acid-doped-PoPDs: (a) FT-IR spectra and (b) XRD patterns.

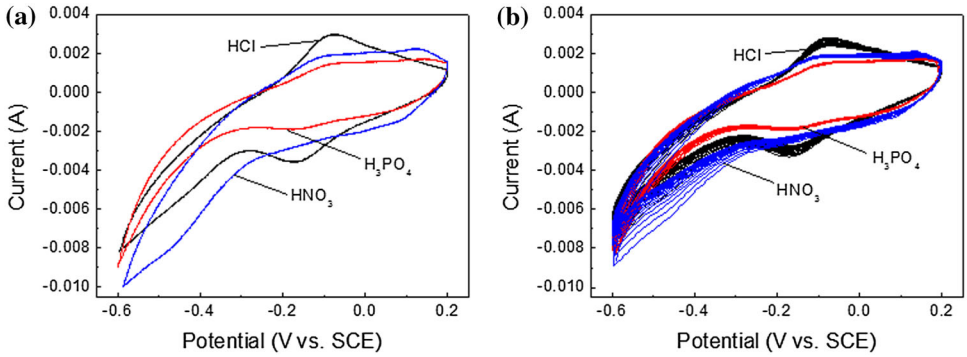

Fig. 2. CVs of different acid-doped PoPD on carbon paper in aqueous 1 M HCl at a scan rate of 0.1 V/s. (a) Initial cyclic voltammograms and (b) 20 cyclic voltammograms.

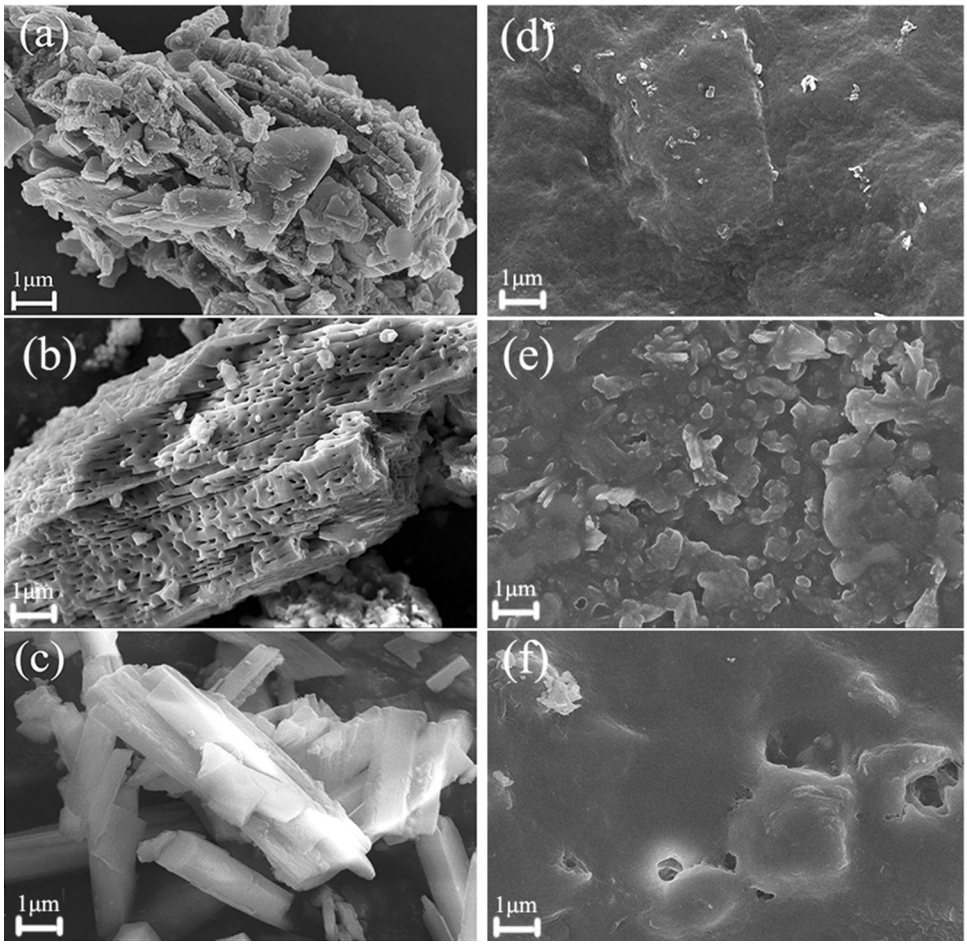

Fig. 3. SEM morphologic of doped-PoPD. (a) HCl, (b) HNO_3, (c) H_3PO_4, (d) PoPD–HCl coating, (e) PoPD–HNO_3 coating, and (f) PoPD–H_3PO_4 coating.

certain depth of depression inside. Figure 3b shows that the surface of PoPD–HNO_3 was relatively uniform with no surface irregularities. PoPD–HNO_3 showed a block structure having a length of around 19 μm and large number of micropores. The SEM image of PoPD–H_3PO_4 in Fig. 3c showed a rectangular parallelepiped structure with a length ranging from 1.5 μm to 9.5 μm and width ranging from 0.3 μm to 1.4 μm.

Corrosion Protection Performance

The corrosion performances of steel samples coated with acid-doped PoPD, including acids such as hydrochloric, nitric, and phosphoric acid, were investigated in 3.5% NaCl solution. To obtain more information regarding the quality of protection, the category of inhibitor, and its effect on the kinetic parameters of anodic and cathodic reactions,

potentiodynamic polarization techniques were employed. In this technique, the corrosion current density (i_{corr}) and corrosion potential (E_{corr}) are obtained using Tafel extrapolation for each dopant studied. The relative protection performances were correlated by comparing the polarization curves of different polymer coatings under the same conditions. Figure 4a shows Tafel polarization curves for mild steel in 3.5% NaCl solution in the absence and presence of various dopant coatings. Values for the E_{corr}, i_{corr}, and corrosion rate are listed in Table I.

The Tafel polarization curves for PoPD–HCl-, PoPD–H_3PO_4-, and PoPD–HNO_3-coated mild steel are shown in Fig. 4a. Generally, the corrosion current density and corrosion potential are associated with the sensitivity or stability of the material to corrosion in a corrosive environment. A low corrosion current density and high corrosion potential imply excellent corrosion resistance of the coating.[34] The i_{corr} decreased from 1.91×10^{-5} A/cm^2 for bare mild steel to 2.05×10^{-6} A/cm^2 for PoPD–HNO_3-coated steel. The E_{corr} of PoPD–HNO_3-coated steel is higher than that of bare steel. The E_{corr} of bare steel is − 0.90 V, while the E_{corr} of PoPD–HNO_3-coated steel reached − 0.76 V. Compared with bare steel, the E_{corr} of the PoPD–HNO_3 coating increased by 0.14 V, and the corrosion current decreased by 1.71×10^{-6} A/cm^2. Table I shows that the i_{corr} values of the PoPD–HCl coating (6.61×10^{-6} A/cm^2) and PoPD–H_3PO_4 coating (4.51×10^{-6} A/cm^2) were less than those of bare mild steel. The E_{corr} values of PoPD–HCl and PoPD–H_3PO_4 coatings increased from − 0.90 V (for bare steel) to − 0.88 V and − 0.83 V, respectively. The exchange current density of PoPD–HNO_3-coated steel was also three times lower than that of bare mild steel. These results suggested that the PoPD–HNO_3 coating on steel formed a protective layer on MS and showed improved corrosion inhibition characteristics.

The porosity of the coating as well as the diffusivity and adhesion between the coating and substrate can affect the corrosion resistance of the coating. A porous coating can lead to erosion of the substrate in corrosive medium and then accelerate the electrochemical dissolution of the substrate.[35] The extent to which the coating corrodes can be judged by the corrosion rate C_R using Eq. 1, the values of which are given in Table II.[36]

$$C_R = 3270 \times \frac{M\,(\mathrm{g}) \cdot i_{corr}\,(\mathrm{A/cm^2})}{n \cdot \rho\,(\mathrm{g/cm^3})} \quad (1)$$

In the above equation, M is the molecular weight of the metal substrate, i_{corr} is the corrosion current, n is the number of electrons lost during the oxidation reaction, and ρ is the average density of the substrate. Some pinholes and holes in the coating can weaken the adhesion of the material at the interface. Such a defect can provide an invasive path for the corrosive medium and increase the area of corrosion. A lower C_R value indicated that the PoPD–HNO_3 coating hindered the passage of electrolytes into the steel substrate because of the increased corrosion resistance. Furthermore, the presence of a polymer could inhibit the reactions at the anode and cathode, such as dissolution at the anode and hydrogen evolution at the cathode.[3,35]

Similar to potentiodynamic polarization, EIS is also a powerful method for evaluating the anticorrosion properties of coatings used in industry.[37–39] Figure 4b shows the Nyquist impedance plot of the coatings after immersion in 3.5% NaCl for 7 days at room temperature. The choice of an equivalent circuit is decided by the Chi-square value and the sum of the square values. The impedance curve in Fig. 4b shows a non-ideal arc shape, and hence the constant phase component (CPE) in the equivalent circuit of Fig. 5 replaced the pure capacitor. This showed a non-uniform impaired coating and non-ideal capacitive behavior. Carbon steel and PoPD with different dopants corresponded to circuit 1 and circuit 2, respectively. The fitting curves are shown in Fig. 4b, and these circuits showed good fitting results. The formula for the impedance of CPE Z_{CPE} is shown in Eq. 2.[37]

$$Z_{CPE} = \frac{1}{Y_0(j\omega)^n} \quad (2)$$

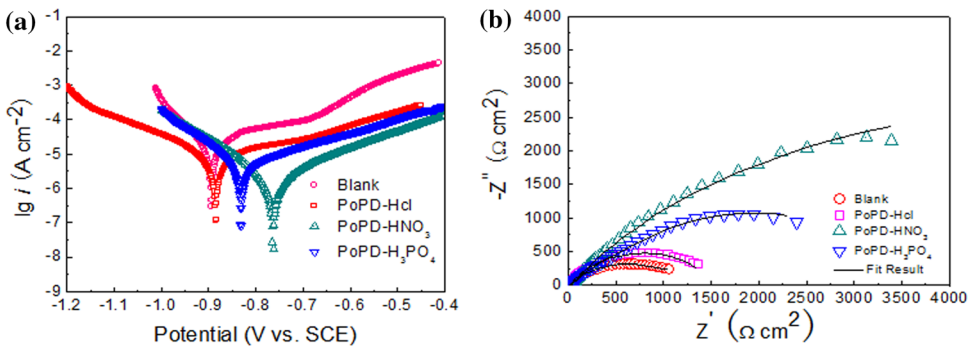

Fig. 4. Behavior of dopant categories on the curves of doped PoPD coatings in 3.5% NaCl solution after being immersed 7 days. (a) Potentiodynamic polarization and (b) Nyquist impedance plots.

Table I. Corrosion kinetic parameters of PoPD-dopant coating samples in 3.5% NaCl solutions after being immersed 7 days. "±"shows the standard deviation

Samples	i_{corr} (μA cm^{-2})	$-E_{corr}$ (V vs. SCE)	C_R (mm/year)
Blank	19.1 ± 0.62	0.90 ± 0.01	0.223 ± 0.007
PoPD–HCl	6.61 ± 0.47	0.88 ± 0.02	0.077 ± 0.005
PoPD–H_3PO_4	4.51 ± 0.31	0.83 ± 0.05	0.053 ± 0.003
PoPD–HNO_3	2.05 ± 0.12	0.76 ± 0.04	0.024 ± 0.001

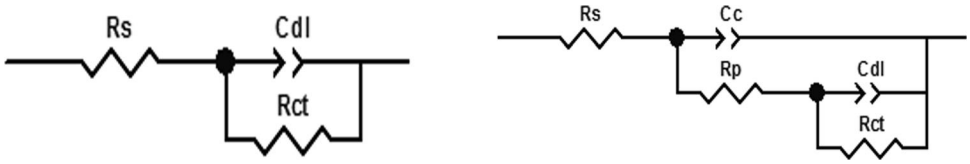

Fig. 5. Equivalent electrical circuits used to model the EIS experiments for mild steel (circuit 1) and PoPD with different dopant coatings (circuit 2).

Table II. Parameters of the equivalent circuit for PoPD-dopant coatings in 3.5% NaCl solution after being immersed 7 days

Samples	R_s (Ω cm^2)	R_p (Ω cm^2)	C_c (F cm^{-2})	R_{ct} (Ω cm^2)	C_{dl} (F cm^{-2})	IE (%)	Chi-square
Bear steel	13.53	NA	NA	1534	0.0017416	NA	6.81×10^{-3}
PoPD–HCl	18.71	1335	0.0010989	1759	0.0015591	12.79	6.42×10^{-3}
PoPD–H_3PO_4	23.71	1761	0.00091061	1905	0.0016499	19.48	5.50×10^{-3}
PoPD–HNO_3	21.09	7045	0.00090823	3624	0.0014263	57.67	8.91×10^{-3}

Here, Y_0, j, and ω corresponded to the admittance magnitude of the CPE, imaginary unit, and angular frequency, respectively. n = 1 corresponded to the ideal capacitance, and, in other cases, the value of n was in the range of 0–1.

The pore resistance–coating capacitance (R_p–C_c) component in the equivalent circuit was dependent on the monomer oxidation and/or polymer deposition on a mild steel substrate, which it formed at the steel/electrolyte interface. The charge transfer resistance-double layer capacitance (R_{ct}–C_{dl}) component was involved in the reaction between the metal and polymer. This could be attributed to iron or other oxidation/reduction reactions occurring in the system as well as the formation of a passive interlayer, where C_{dl} and R_{ct} represented double-layer capacitance and charge transfer resistance, respectively.[35,40] The equivalent circuit data of the coating were fitted by Zview 2.0 software, and the obtained data are presented in Table II.

Pore resistance (R_p) and coating capacitance (C_c) are two electrochemical parameters in EIS that indicate the ability of the coating to resist corrosion. Moreover, C_c is an important standard parameter for coating integrity. It shows the tendency of the electrolyte to absorb the surface coating.[41] For the PoPD–HCl coating, the R_p (1335 Ω cm^2) was lower than those of PoPD–H_3PO_4 (1761 Ω cm^2) and PoPD–HNO_3 (7045 Ω cm^2), which indicated that the coating provided good protection. However, its C_c value was the lowest. This could be attributed to the presence of a relatively dense barrier layer on mild steel. Furthermore, the R_{ct} and C_{dl} values of all the samples showed the same trends as those of their corresponding R_p and C_c values. The highest values of R_p and R_{ct} and the lowest values of C_c and C_{dl} of the PoPD–HNO_3 coating indicated that this coating offered the best corrosion performance to mild steel. The C_{dl} value generally gives an indication of local dielectric constant.[42,43] The water molecules at the site of the coating defect can be replaced by inhibitors such as polymer molecules and chelates on the metal surface, which results in a decrease of the local dielectric constant.[44]

The pores in the coating provide channels for chloride ions and water molecules to penetrate to the coating/metal interface. Through electrochemical reactions, they weaken the adhesion of the layer to the substrate and thus reduce the barrier properties of the PoPD polymer coating. To more intuitively compare the protective properties of the coating, the following Eq. 3 is usually used to calculate the inhibition efficiency (IE%).[45]

$$IE\% = \frac{R_{ct} - R_{ct}^0}{R_{ct}} \times 100 \quad (3)$$

In the equation, R_{ct} and R_{ct}^{0} denote the total charge transfer resistances of the PoPD-dopant coatings and bare mild steel substrate, respectively. The calculated values of IE% are listed in Table II. The inhibition efficiency was increased in the presence of HNO_3 and the IE% reached 58%, which was 3–4.5 times higher than those of the hydrochloric acid and phosphoric acid dopants. The dopant ions present in the polymeric structure affect the corrosion protection mechanism.[46] In general, conductive polymers provide anodic protection by passivating the metal substrate while providing a physical barrier for corrosion protection. When the dopant is gradually released during the inhibition process, the polymer serves as a mechanical barrier in the reduced state. Compared with Cl^-, which is an aggressive ion, the phosphoric acid solution can strongly adhere, forming a complex with Fe. This coating is applied to the metal surface to keep away the corrosive ions from contacting with the substrate, thus effectively protecting the metal surface.[37,46] Nitric acid renders the passive film more resistant by incorporating NO_3^- ions.[47] Furthermore, with a low concentration of NO_3^-, the dopant counterions move in the polymer chain, whereas Cl^- acts as a corrosion inhibitor for freely dissolved iron.[48]

CONCLUSION

Hydrochloric acid-, phosphoric acid-, and nitric acid-doped PoPDs were prepared by oxidative polymerization. The corrosion resistances of mild steel coated with different components of PoPD were determined in 3.5% NaCl. Corrosion behavior was evaluated based on potentiodynamic anodic polarization and impedance measurements from Nyquist plots. The results obtained showed that all three PoPD coatings could provide corrosion resistance to mild steel. Among them, PoPD–HNO_3 showed the best corrosion inhibition, and the corrosion resistance efficiency reached about 60%. It was 3–4.5 times that of the other two acid-doped coatings.

ACKNOWLEDGEMENTS

The authors are grateful for the financial support of the National Natural Science Foundation of China (nos. 51834004, 51774076, 51704063 and 51474057). The first author is also thankful to Liaoning Key Laboratory for Metallurgical Sensor and Technology providing the facilities for the research.

CONFLICT OF INTEREST

The authors declare that they have no conflict of interest.

REFERENCES

1. A. Madhankumar and N. Rajendran, *Synth. Met.* 162, 176 (2012).
2. A. Gebert, K. Buchholz, A. Leonhard, K. Mummert, J. Eckert, and L. Schultz, *Mater. Sci. Eng. A* 267, 294 (1999).
3. S.S.A.E. Rehim, S.M. Sayyah, M.M. El-Deeb, S.M. Kamal, and R.E. Azooz, *Mater. Chem. Phys.* 123, 20–27 (2010).
4. M. Düdükcü, *Res. Chem. Intermed.* 39, 3641 (2013).
5. D.W. Deberry, *J. Electrochem. Soc.* 132, 1022 (1985).
6. T. Patois, B. Lakard, S. Monney, X. Roizard, and P. Fievet, *Synth. Met.* 161, 2498 (2011).
7. K. Cysewska, M. Gazda, and P. Jasinski, *Surf. Coat. Technol.* 328, 248 (2017).
8. S. Biallozor and A. Kupniewska, *Synth. Met.* 155, 443 (2005).
9. M.A. Malika, M.T. Galkowski, H. Bala, B. Grzybowskab, and P.J. Kulesza, *Electrochim. Acta* 44, 2157 (1999).
10. Z. Peng, L. Qiang, and L. Yan, *Appl. Surf. Sci.* 252, 1596 (2005).
11. S. Samanta, P. Roy, and P. Kar, *Macromol. Res.* 24, 342 (2016).
12. J.F. Feng, T. Sun, and J. Zhu, *Synth. Met.* 213, 12 (2016).
13. V.V. Shumyantseva, T.V. Bulko, L.V. Sigolaeva, A.V. Kuzikov, and A.I. Archakov, *Biosens. Bioelectron.* 86, 330 (2016).
14. W. Deng, Y. Zhang, Y. Tan, and M. Ma, *J. Electroanal. Chem.* 787, 103 (2017).
15. L. Ding, Z. Gong, M. Yan, J. Yu, and X. Song, *Microchim. Acta* 184, 4531 (2017).
16. U. Riaz, S.M. Ashraf, R. Raza, K. Kohli, and J. Kashyap, *Ind. Eng. Chem. Res.* 55, 6300 (2016).
17. S. Bilal, A.A. Shah, and R. Holze, *Electrochim. Acta* 56, 3353 (2011).
18. A.A. Ganash, F.M. Al-Nowaiser, S.A. Al-Thabaiti, and A.A. Hermas, *J Solid State Electr.* 17, 849 (2013).
19. A.A. Hermas, Z.X. Wu, M. Nakayama, and K. Ogura, *J. Electrochem. Soc.* 153, 199 (2006).
20. S. Bhadra, D. Khastgir, N.K. Singha, and J.H. Lee, *Prog. Polym. Sci.* 34, 783 (2009).
21. G. Ebrahimi, J. Neshati, and F. Rezaei, *Prog. Org. Coat.* 105, 1 (2017).
22. S. Samanta, P. Roy, and P. Kar, *Polym. Adv. Technol.* 28, 797 (2017).
23. N. Kannapiran, A. Muthusamy, P. Chitra, S. Anand, and R. Jayaprakash, *J. Magn. Magn. Mater.* 423, 208 (2017).
24. V.V. Chabukswar, A.S. Horne, S.V. Bhavsar, K.N. Handore, P.K. Chhattise, S.S. Pandule, D.T. Walunj, and S.U. Shisodia, *J. Macromol. Sci. A* 51, 435 (2014).
25. M. Huang, X. Li, and W. Duan, *Polym. Int.* 54, 70 (2005).
26. L.F. D'Elia, R.L. Ortíz, O.P. Márquez, J. Márquez, and Y. Martínez, *J. Electrochem. Soc.* 148, 297 (2001).
27. S.Ü. Çelik, A. Aslan, and A. Bozkurt, *Solid State Ion.* 179, 683 (2008).
28. W.J. Liang, S.J. Hsieh, C.Y. Hsu, W.F. Chen, and P.L. Kuo, *J. Polym. Sci. Pol. Phys.* 44, 2135 (2006).
29. S. Ashokan, V. Ponnuswamy, P. Jayamurugan, J. Chandrasekaran, and Y.V. Subba Rao, *Superlattices Microstruct.* 85, 282 (2015).
30. K.R. Reddy, K.P. Lee, and A.I. Gopalan, *Colloids Surf. A* 320, 49 (2008).
31. J. Qiao, N. Yoshimoto, M. Ishikawa, and M. Morita, *Solid State Ion.* 156, 415 (2003).
32. E. Vilarrasa-García, J.A. Cecilia, M. Bastos-Neto, C.L. Cavalcante Jr, D.C.S. Azevedo, and E. Rodríguez-Castellón, *Appl. Surf. Sci.* 410, 315 (2017).
33. P. Muthirulan and N. Rajendran, *Surf. Coat. Technol.* 206, 2072 (2012).
34. R.M. Bandeira, J.V. Drunen, G. Tremiliosi-Filho, D.S. José-Ribeiro, and D.M. José Milton Elias, *Prog. Org. Coat.* 106, 50 (2017).
35. V.P. Shinde and P.P. Patil, *J Solid State Electr.* 17, 29 (2013).
36. H. Huang, T. Huang, T. Yeh, C. Tsai, C. Lai, M. Tsai, J. Yeh, and Y. Chou, *Polymer* 52, 11 (2011).
37. L. Jiang, J.A. Syed, Y. Gao, Q. Zhang, J. Zhao, H. Lu, and X. Meng, *Appl. Surf. Sci.* 426, 87 (2017).
38. M. Naseri, L. Fotouhi, and A. Ehsani, *J. Electrochem. Sci. Technol.* 9, 28 (2018).

39. R. Solmaz, *Corros. Sci.* 52, 3321 (2010).
40. K. Cysewska, L.F. Macía, P. Jasiński, and A. Hubin, *Electrochim. Acta* 290, 520 (2018).
41. P. Sambyal, G. Ruhi, H. Bhandari, and S.K. Dhawan, *Surf. Coat. Technol.* 272, 129 (2015).
42. N. Soltani, N. Tavakkoli, M. Khayatkashani, M.R. Jalali, and A. Mosavizade, *Corros. Sci.* 62, 122 (2012).
43. H. Ashassi-Sorkhabi, B. Shaabani, and D. Seifzadeh, *Electrochim. Acta* 50, 3446 (2005).
44. H. Akhavan, M. Izadi, I. Mohammadi, T. Shahrabi, and B. Ramezanzadeh, *J. Electrochem. Soc.* 165, 670 (2018).
45. M. Beikmohammadi, L. Fotouhi, A. Ehsani, and M. Naseri, *Solid State Ion.* 324, 138 (2018).
46. A.A. Shah, S. Bilal, and R. Holze, *Synth. Met.* 162, 356 (2012).
47. B. Laurent, N. Gruet, B. Gwinner, F. Miserque, K. Rousseau, and K. Ogle, *Electrochim. Acta* 258, 653 (2017).
48. N.N. Khobragade, A.V. Bansod, and A.P. Patil, *Mater. Res. Express* 5, 046526 (2018).